



ELSEVIER

Nuclear Physics A 594 (1995) 325–345

NUCLEAR  
PHYSICS A

# Chiral dynamics and the low-energy kaon–nucleon interaction<sup>\*</sup>

N. Kaiser, P.B. Siegel<sup>1</sup>, W. Weise*Physik Department, Technische Universität München, Institut für Theoretische Physik, D-85747 Garching, Germany*

Received 6 May 1995; revised 3 August 1995

---

## Abstract

We examine the meson–baryon interaction in the strangeness  $S = -1$  sector using an effective chiral Lagrangian. Potentials are derived from this Lagrangian and used in a coupled-channel calculation of the low-energy observables. The potentials are constructed such that in the Born approximation the  $s$ -wave scattering length is the same as that given by the effective chiral Lagrangian, up to order  $q^2$ . A comparison is made with the available low-energy hadronic data of the coupled  $K^-p$ ,  $\Sigma\pi$ ,  $\Lambda\pi$  system, which includes the  $\Lambda(1405)$  resonance,  $K^-p$  elastic and inelastic scattering, and the threshold branching ratios of the  $K^-p$  decay. Good fits to the experimental data and estimates of previously unknown Lagrangian parameters are obtained.

---

## 1. Introduction

The effective chiral Lagrangian including baryons, which corresponds to an expansion in increasing powers of derivatives of the meson fields and quark masses, has been successful in understanding many properties of the meson–baryon system at low energies [1]. Since the pion mass is small, properties of the pion–nucleon system are well described close to threshold. Recently, the  $SU(3)$  chiral Lagrangian has also been applied to the  $K^+N$  system [2,3]. In both the  $\pi N$  and  $K^+N$  cases, the low-energy ( $s$ -wave) interaction is relatively weak and the leading term of the Lagrangian (linear in the meson four-momentum  $q$ ) is the main one. In this article we examine the  $\bar{K}N$  system within the context of the effective chiral Lagrangian. In contrast to the  $\pi N$  and

---

<sup>\*</sup> Work supported in part by BMBF and GSI.

<sup>1</sup> On sabbatical leave from the California State Polytechnic University, Pomona, CA 91768, USA.

$K^+N$  cases, the  $\bar{K}N$  system is a strongly interacting multichannel system with an s-wave resonance, the  $\Lambda(1405)$ , just below the  $K^-p$  threshold. Terms of higher order in  $q$  will therefore play a more pronounced role in the interaction. In fact the dynamical generation of such a resonance necessarily leads beyond any finite order expansion of chiral perturbation theory.

The motivation for nevertheless applying the effective chiral Lagrangian to the  $K^-N$  system is two-fold: firstly, to explore whether it provides driving terms with a sufficiently strong attraction to generate a resonance at the right energy; secondly, to test the theory in the  $S = -1$  sector and to obtain information about the parameters of the Lagrangian not accessible in the  $\pi N$  or  $K^+N$  interactions. At low energies, the  $K^-$  and proton can scatter into six different  $\bar{K}N$  and pion-hyperon channels, and the data place constraints on the relative interaction strengths among the different channels. Since each of the different terms of the chiral Lagrangian has its own particular  $SU(3)$  structure, this six-channel system is a good testing ground for the theory and enables one to obtain estimates of the Lagrangian parameters.

The presence of the  $\Lambda(1405)$  resonance requires that one needs to go to infinite order in a certain class of rescattering diagrams. Thus to build up the resonance we are led to constructing a potential model to handle the calculation. A potential model was previously applied to the  $\bar{K}N$  system [4], and the approximations necessarily involved in using this method are expected to be quite reasonable, since the resonance dominates the interaction. In order to connect the chiral Lagrangian to the potential model approach, we construct a meson-baryon potential which in the Born approximation has the same s-wave scattering length as the effective chiral Lagrangian, up to order  $q^2$ . Two different forms of the potential, one local and one separable, are investigated. This potential is iterated in a Lippmann-Schwinger equation, and the free parameters of the Lagrangian are adjusted to fit a wide variety of low-energy data of the kaon-baryon system. An additional constraint is placed on the parameters so that the isospin-even  $\pi N$  s-wave scattering length is consistent with its experimental value. We find that parameters from Lagrangian terms up to order  $q^2$  are sufficient to fit the data. In particular, the observed properties of the  $\Lambda(1405)$  resonance are reproduced remarkably well. Furthermore, as a consistency check, we calculate the  $KN$  s-wave phase shift (strangeness  $S = +1$  sector) from the parameters obtained in fitting the  $\bar{K}N$  system.

In the second section we describe the effective chiral Lagrangian and the potential model, and in the third section we discuss our results. In each section we consider interaction terms of order  $q$  and then of order  $q^2$ , where  $q$  stands for the meson four-momentum. In the final section we discuss the limitations and some qualitative aspects of the calculation.

## 2. Effective chiral Lagrangian

The effective low-energy Lagrangian density for interacting systems of pseudoscalar mesons and baryons can be written generally as [5,6]

$$\mathcal{L} = \mathcal{L}^{(1)} + \mathcal{L}^{(2)} + \dots \tag{1}$$

corresponding to an increasing number of derivatives (external momenta) and quark masses.

### 2.1. Leading order term

In the relativistic formalism the leading order term [5,6] is given by

$$\begin{aligned} \mathcal{L}^{(1)} = & \text{tr} (\bar{\Psi}_B (i\gamma_\mu D^\mu - M_0) \Psi_B) + F \text{tr} (\bar{\Psi}_B \gamma_\mu \gamma_5 [A^\mu, \Psi_B]) \\ & + D \text{tr} (\bar{\Psi}_B \gamma_\mu \gamma_5 \{A^\mu, \Psi_B\}), \end{aligned} \tag{2}$$

with the chiral covariant derivative

$$D^\mu \Psi_B = \partial^\mu \Psi_B + [\Gamma^\mu, \Psi_B], \tag{3}$$

and

$$\Gamma^\mu = \frac{1}{8f^2} [\phi, \partial^\mu \phi] + \mathcal{O}(\phi^4). \tag{4}$$

The matrices  $\Psi_B$  and  $\phi$  represent the octet baryon Dirac fields and the octet pseudoscalar meson fields, respectively (see Appendix A),  $f \simeq 90$  MeV is the pseudoscalar meson decay constant and  $M_0$  the baryon mass in the chiral limit [7]. The constants  $F$  and  $D$  are the SU(3) axial vector couplings, whose accepted values are  $F \simeq 0.5$  and  $D \simeq 0.75$  [8], together with  $g_A = F + D$ . Through Goldberger–Treiman relations they determine the pseudovector meson–baryon coupling strengths.

The interaction part involving the covariant derivative can be expanded, and to leading order in the external meson four-momentum  $q$  is given by

$$\mathcal{L}_{\text{int}}^{(1)} = \frac{i}{8f^2} \text{tr} (\bar{B} [ [\phi, \partial_0 \phi], B ]), \tag{5}$$

where the field  $B$  is the “large component” of the Dirac spinor  $\Psi_B$ , defined via  $\Psi_B = \exp(-iM_0 v \cdot x) [B + \mathcal{O}(1/M_0)]$  [9,10]. The four-velocity  $v$  permits fixing a particular reference frame which we choose to be the meson–baryon center-of-mass system. An observer in that frame is characterized by  $v^\mu = (1, 0, 0, 0)$ . This part of the interaction, Eq. (5), is the current algebra, or the Weinberg–Tomozawa, term [11]. The tree approximation of this term agrees with the experimental values of the s-wave scattering length to within 15% for  $\pi N$  and to within 50% for the  $K^+ N$  system. In the  $K^+ p$  channel this Weinberg–Tomozawa term is repulsive. The Lagrangian also applies to the  $K^- N$  interaction. Here, the current algebra term produces an attractive interaction. The  $\Lambda(1405)$  resonance just below the  $K^- p$  threshold could be resulting from this attractive term. We investigate this possibility in the next section.

## 2.2. Order $q^2$ terms

In addition to the order  $q$  terms mentioned above, the tree graphs of the relativistic Lagrangian  $\mathcal{L}^{(1)}$  give rise to s-wave meson–baryon amplitudes at order  $q^2$  (and higher). These order  $q^2$  terms are relativistic ( $1/M_0$ ) corrections from the covariant-derivative piece and the Born graphs involving the axial coupling terms ( $F$  and  $D$ ). In addition to these order  $q^2$  pieces, we have to consider the most general form of the chiral effective Lagrangian  $\mathcal{L}^{(2)}$ . The complete relativistic version involving all terms allowed by chiral symmetry can be found in Ref. [6]. In the heavy baryon formalism its form is simpler, and the relevant s-wave terms are [3]<sup>2</sup>

$$\begin{aligned} \mathcal{L}^{(2)} = & b_D \text{tr}(\bar{B}\{\chi_+, B\}) + b_F \text{tr}(\bar{B}[\chi_+, B]) + b_0 \text{tr}(\bar{B}B) \text{tr}(\chi_+) \\ & + d_D \text{tr}(\bar{B}\{A^2 + (v \cdot A)^2, B\}) + d_F \text{tr}(\bar{B}[A^2 + (v \cdot A)^2, B]) \\ & + d_0 \text{tr}(\bar{B}B) \text{tr}(A^2 + (v \cdot A)^2) \\ & + d_1 [\text{tr}(\bar{B}A_\mu) \text{tr}(A^\mu B) + \text{tr}(\bar{B}(v \cdot A)) \text{tr}((v \cdot A)B)] \\ & + d_2 \text{tr}(\bar{B}[A_\mu B A^\mu + (v \cdot A)B(v \cdot A)]) + \dots, \end{aligned} \quad (6)$$

where

$$\chi_+ = -\frac{1}{4f^2} \{\phi, \{\phi, \chi\}\}. \quad (7)$$

The matrix  $\chi$  is proportional to the quark mass matrix and has only diagonal elements (see Appendix A). Using the Gell-Mann, Oakes, Renner relation in the isospin limit for the pseudoscalar mesons, the diagonal elements of  $\chi$  are  $(m_\pi^2, m_\pi^2, 2m_K^2 - m_\pi^2)$ . The axial matrix operator  $A$  is given by

$$A_\mu = -\frac{1}{2f} \partial_\mu \phi + \mathcal{O}(\phi^3). \quad (8)$$

All contributions of  $\mathcal{L}^{(2)}$  at tree level are of order  $q^2$ . The next order  $q^3$  involves loops. The amplitudes for all channel couplings up to order  $q^2$ , which also include the relativistic corrections, are given in Appendix B.

The constants in front of the various terms are not determined from chiral symmetry, but need to be determined from experiment. The first two,  $b_D$  and  $b_F$ , can be determined from the baryon mass splittings since to order  $q^2$

$$m_\Sigma - m_\Lambda = \frac{16}{3} b_D (m_K^2 - m_\pi^2), \quad m_\Xi - m_N = 8 b_F (m_\pi^2 - m_K^2). \quad (9)$$

One obtains  $b_D = +0.066 \text{ GeV}^{-1}$  and  $b_F = -0.213 \text{ GeV}^{-1}$ . Data restricts the range for the constant  $b_0$ , since it is related to the  $\pi N$  sigma term. To order  $q^2$  we have

$$\sigma_{\pi N} = -2m_\pi^2 (b_D + b_F + 2b_0), \quad (10)$$

<sup>2</sup> Terms proportional to the difference  $(v \cdot A)^2 - A^2$  which have independent coefficients contribute only in p-waves and are therefore not included here.

and the strangeness content of the proton to this order is given by

$$\frac{\langle p | \bar{s}s | p \rangle}{\langle p | \bar{u}u + \bar{d}d | p \rangle} = \frac{b_0 + b_D - b_F}{2b_0 + b_D + b_F}. \quad (11)$$

Thus,  $b_0$  cannot be greater than  $-0.28 \text{ GeV}^{-1}$  since otherwise the strangeness content of the proton would be negative. We also did not allow  $b_0$  to be less than  $-0.52 \text{ GeV}^{-1}$ , which keeps  $\sigma_{\pi N}$  less than about 45 MeV [12]. Data from interactions among the meson–baryon octet (i.e. the  $K^-N$  interaction) gives information regarding the double-derivative parameters, the  $d$  terms in Eq. (6). The notation in Eq. (6) was adopted since if  $\chi$  is proportional to the unit matrix (i.e.  $m_u = m_d = m_s$ ), terms with the same subscripts have the same relative SU(3) strengths.

### 2.3. The pseudo-potential

The motivation for studying the  $K^-N$  system is to see how well the effective chiral Lagrangian describes the experimental data in this strangeness sector, and to obtain estimates for the “ $d$ ” parameters of Eq. (6). Since the interaction supposedly produces a resonance just below the  $K^-p$  threshold, a certain class of diagrams needs to be summed to infinite order to produce a pole at the appropriate energy. Thus, the chiral perturbation expansion for the scattering amplitude is not feasible, and we adopt a potential model approach. We connect the two formalisms in the following way: *the pseudo-potentials are constructed such that up to order  $q^2$  they have, in the Born approximation, the same  $s$ -wave scattering length as the chiral Lagrangian.* In the last section we discuss some of the limitations of using this potential approach.

The above prescription for obtaining a potential from the chiral Lagrangian gives a unique zero-range potential of the form

$$V_{ij}(\mathbf{r}) = \frac{C_{ij}}{2f^2} \sqrt{\frac{M_i M_j}{s\omega_i \omega_j}} \delta^3(\mathbf{r}), \quad (12)$$

where the  $i$  and  $j$  label the six meson–baryon channels ( $\pi^+\Sigma^-, \pi^0\Sigma^0, \pi^-\Sigma^+, \pi^0\Lambda, K^-p, \bar{K}^0n$ ). Here  $\sqrt{s}$  is the total center-of-mass energy of the system,  $M_i$  is the mass of the baryon in channel  $i$ , and  $\omega_i$  is the reduced energy of channel  $i$  in the center-of-mass frame. Explicitly,

$$\omega_i = \frac{E_i \sqrt{E_i^2 + M_i^2 - m_i^2}}{E_i + \sqrt{E_i^2 + M_i^2 - m_i^2}}, \quad (13)$$

where  $m_i$  is the mass and  $E_i$  is the energy of the meson in channel  $i$ . The  $C_{ij}$  are determined directly from the effective chiral Lagrangian and are given in Appendix B. The kinematic factor  $\sqrt{M_i M_j / s\omega_i \omega_j}$  is needed to obtain the proper relativistic flux factor in the differential cross section. The differential cross section from initial channel  $j$  to final channel  $i$  in the Born approximation is

$$\begin{aligned} \left( \frac{d\sigma_{ij}}{d\Omega_{\text{c.m.}}} \right)_{\text{Born}} &= \frac{k_i}{k_j} \left| \frac{\sqrt{\omega_i \omega_j}}{2\pi} \int \exp[-i(\mathbf{k}_j - \mathbf{k}_i) \cdot \mathbf{r}] V_{ij}(r) d^3r \right|^2 \\ &= \frac{k_i}{k_j} \frac{M_i M_j}{16\pi^2 s} \frac{|C_{ij}|^2}{f^4}, \end{aligned} \quad (14)$$

where we have used Eq. (12) in the last step, and  $k_i$  stands for the meson momentum in the center-of-mass frame.

In order to dynamically produce the  $\Lambda(1405)$  resonance, the potential must be iterated to infinite order. Here we use a Lippmann–Schwinger equation. To obtain a finite result, a cutoff or inverse range scale, denoted by  $\alpha$ , needs to be introduced in the potential. We examine two ways of parameterizing the finite range of the potential while keeping the Born term the same: a local potential and one separable in the incoming and outgoing relative momenta. For the local potential between channel  $i$  and  $j$  we use a Yukawa form:

$$V_{ij}(r) = \frac{C_{ij} \alpha_{ij}^2}{8\pi f^2} \sqrt{\frac{M_i M_j}{s \omega_i \omega_j}} \frac{e^{-\alpha_{ij} r}}{r}, \quad (15)$$

where  $r = |\mathbf{r}|$ . In our analysis, we found a satisfactory solution for the local potential using only a single common range parameter  $\alpha = 412$  MeV for all channels. For the Yukawa potential the parameter  $\alpha$  can be interpreted as an average “effective mass” that represents the spectrum of exchanged particles in the  $t$ -channel mediating the interaction. The value of  $\alpha$  found here for the  $l = 0$  channel is reminiscent of typical two-pion ranges.

For comparison we also examine a separable potential of the momentum space form:

$$V_{ij}(k_i, k_j) = \frac{C_{ij}}{4\pi^2 f^2} \sqrt{\frac{M_i M_j}{s \omega_i \omega_j}} \frac{\alpha_i^2}{\alpha_i^2 + k_i^2} \frac{\alpha_j^2}{\alpha_j^2 + k_j^2}, \quad (16)$$

where  $k_i$  is the center-of-mass momentum for channel  $i$ . The potentials are inserted into a Lippmann–Schwinger equation. For the local potential, this equation is solved in coordinate space:

$$\nabla^2 \psi_i + k_i^2 \psi_i = 2\omega_i \sum_j V_{ij} \psi_j. \quad (17)$$

For the separable potential we use the Lippmann–Schwinger equation (for the  $s$ -wave) in momentum space:

$$T_{ij}(k_i, k_j) = V_{ij}(k_i, k_j) + \sum_n \int_0^\infty \frac{q^2 dq 2\omega_n V_{in}(k_i, q) T_{nj}(q, k_j)}{k_n^2 - q^2 + i\epsilon}, \quad (18)$$

which can then be solved analytically. The  $T$ -matrix resulting from this equation is related to the nonrelativistic scattering amplitude  $f_{ij} = -\pi \sqrt{\omega_i \omega_j} T_{ij}$ . The total  $s$ -wave cross section for the channel  $j \rightarrow i$  is thus given by

$$\sigma_{ij} = 4\pi^3 \frac{k_i}{k_j} \omega_i \omega_j |T_{ij}|^2. \quad (19)$$

Keeping only the Born term and using a zero-range potential, i.e.  $\alpha_i = \infty$ , this cross section becomes

$$\sigma_{ij}^{\text{Born}} = 4\pi \frac{k_i M_i M_j}{k_j 16\pi^2 s} \frac{|C_{ij}|^2}{f^4}, \quad (20)$$

which agrees with the result of Eq. (14).

For our applications, the local potential is the more physical one, since it permits an interpretation in terms of t-channel exchange processes. For example, vector meson exchange has the same basic SU(3) structure as the current algebra term. However, it is useful also to examine the separable potential for a qualitative analysis and to check for model dependencies. As will be shown in the next section, the results of our analysis and the values of the “d” parameters turn out to be very similar for the two different potentials. Hence the physics described here is not sensitive to the specific form of the potential.

### 3. Results

Since the Weinberg–Tomozawa (current algebra) term is known to be the largest one in the s-wave  $\pi N$  interaction, it is instructive to examine how well the interaction due to this term alone reproduces the available data in the  $S = -1$  sector. So we start by examining the current algebra term by itself first, and then add terms involving order  $q^2$  in the chiral Lagrangian.

#### 3.1. Current algebra term at lowest order

The potential for this term is obtained by setting all the “b” and “d” parameters to zero in  $C_{ij}$  and neglecting the relativistic corrections in Eq. (2). The only free parameters are the inverse ranges  $\alpha_i$ . First we investigate if the current algebra term alone will produce a resonance or quasi-bound state. To do this, we use a common range  $\alpha$  for all channels. The results are shown in Table 1, where we list the energy of the quasi-bound state formed for different parameters  $\alpha$ . As can be seen, if the range parameter of the interaction for the local potential is larger than 300 MeV then a quasi-bound state is indeed formed below the  $K^-p$  threshold. The range of the interaction is roughly 0.7 fm. For the separable potential, the same resonance below the  $K^-p$  threshold is produced for a value of  $\alpha$  greater than 400 MeV.

Thus, a potential derived from chiral dynamics with interaction ranges commensurate with the meson–baryon system *necessarily produces a quasi-bound state or resonance below or near the  $K^-p$  threshold.*

How well does the current algebra piece predict the other low-energy data? First we consider the scattering data. We have performed a  $\chi^2$  analysis on the low-energy scattering data [13–17] as follows: first a common range  $\alpha$  was picked, then the value of the decay constant  $f$  was determined to produce a resonance at 1405 MeV. Then

Table 1

The energy of the  $\bar{K}N$  ( $I = 0$ ) quasi-bound state produced from the current algebra (Weinberg–Tomozawa) term alone as a function of the range parameter  $\alpha$  for both the local and the separable potential. The range  $\alpha$  is the same for all channels

Local potential		Separable potential	
$\alpha$ (MeV)	energy (MeV)	$\alpha$ (MeV)	energy (MeV)
550	<1300	700	<1300
500	1336	600	1367
450	1378	550	1405
400	1417	500	1424
350	1431	450	1431
300	1434	400	1434

the total cross sections were calculated, compared with the available experimental data, and a chi-square per data point,  $\chi^2/N$ , was determined. The parameter  $\alpha$  was varied until  $\chi^2/N$  was minimized. Note that since the energy is low, only the  $l = 0$  partial wave needs to be considered. The results are shown in Table 2. We see that for both potentials, a fairly good fit,  $\chi^2/N = 2.0$ , to the scattering data is possible. For the local potential, the minimum came out to be at  $f = 90$  MeV, which almost coincides with the pseudoscalar meson decay constant in the chiral limit. It is quite remarkable that the current algebra term alone, when iterated using a common off-shell range parameter, gives agreement with six scattering channels and produces an  $I = 0$  resonance at 1405 MeV. For the separable potential, a  $\chi^2$  minimum was found at  $f = 110$  MeV.

For the  $K^+N$   $S = +1$  sector, the un-iterated current algebra term gives zero for the  $I = 0$  and  $-0.585$  fm for the  $I = 1$  s-wave scattering length. Experimentally, the  $I = 0$  scattering length is indeed very small. To obtain the experimental value of  $-0.32$  fm for the  $I = 1$  scattering length, range parameters  $\alpha = 600$  MeV for the local and  $\alpha = 557$  MeV for the separable potential were needed.

In examining the threshold branching ratios, the situation is not so good for the current algebra term alone. The hadronic threshold branching ratios are [18,19]

$$\gamma = \frac{\Gamma(K^-p \rightarrow \pi^+\Sigma^-)}{\Gamma(K^-p \rightarrow \pi^-\Sigma^+)} = 2.36 \pm 0.04,$$

Table 2

Best-fit results using only the current algebra term for the local and separable potential. The  $\chi^2$  per data point is only for the elastic and inelastic  $K^-p$  scattering data. In both cases a resonance is formed at 1405 MeV. The experimental value for  $\gamma$  is  $2.36 \pm 0.04$

Potential	$\alpha$ (MeV)	$f$ (MeV)	$\chi^2/N$ (for scattering data)	$\gamma$	$R_c$	$R_n$
local	395	90	1.8	1.34	0.645	0.15
separable	700	110	1.8	1.21	0.652	0.14
experiment				2.36 $\pm 0.04$	0.66 $\pm 0.011$	0.19 $\pm 0.015$



$$R_c = \frac{\Gamma(K^-p \rightarrow \text{charged particles})}{\Gamma(K^-p \rightarrow \text{all})} = 0.664 \pm 0.011, \quad (21)$$

$$R_n = \frac{\Gamma(K^-p \rightarrow \pi^0\Lambda)}{\Gamma(K^-p \rightarrow \text{all neutral states})} = 0.189 \pm 0.015.$$

They place tight constraints on the relative potential strengths of the  $\bar{K}N$  system. Two of the branching ratios are in fair agreement with experiment; however, the strangeness plus double charge exchange branching ratio  $\gamma$  is far off. Experimentally, the channel  $\pi^+\Sigma^-$  is produced 2.4 times as often as  $\pi^-\Sigma^+$  in the decay at threshold. Note that the current algebra piece in lowest order gives zero for the  $K^-p \rightarrow \pi^+\Sigma^-$  interaction. In terms of chiral power counting, the numerator goes as  $q^4$  and the denominator as  $q^2$ , and the ratio  $\gamma$  is formally suppressed. Experimentally this is not the case, which demonstrates the limits of using a chiral perturbation expansion for the low-energy  $\bar{K}N$  system.

We let the ranges vary for each channel to see if it was possible to fit both the scattering data and the three threshold branching ratios. No fit was found. Next we examine if it is possible to match the data by including the terms of order  $q^2$ .

### 3.2. Order $q^2$ terms

One cannot vary  $b_0$  and the “ $d$ ” parameters arbitrarily to fit the  $\bar{K}N$  data, since the chiral Lagrangian applies to all meson–baryon interactions. For two  $s$ -wave scattering lengths ( $I = 0$   $\bar{K}N$  and isospin-even  $\pi N$ ) the current algebra term gives zero and the leading term is order  $q^2$ . Experimentally, these scattering lengths are small:  $a_{\pi N}^+ = -(0.012 \pm 0.006)$  fm [20] and  $a_{\bar{K}N}^0 = -(0.02 \pm 0.04)$  fm [21]. Since  $b_0$  and the “ $d$ ” parameters are the leading terms for these two scattering lengths, we restrict their values in the search to be compatible with the experimental results. The  $\pi N$  isospin-even and  $I = 0$   $\bar{K}N$  scattering lengths are given in Appendix B to order  $q^3$  and  $q^2$ , respectively. For the  $I = 1$   $\bar{K}N$  scattering length, the range in the potential can be adjusted to fit the experimental value of  $-0.32$  fm.

The search was done as follows: First the nine parameters  $b_0$ ,  $d_0$ ,  $d_D$ ,  $d_F$ ,  $d_1$ ,  $d_2$  and the range(s) were chosen. Then a value for  $f$  was determined which produced a resonance at 1405 MeV. The total  $\chi^2$  for the scattering data to the six channels, the three threshold branching ratios, and the scattering lengths  $a_{\pi N}^+$  and  $a_{\bar{K}N}^0$  was calculated. In order to have the pion decay constant  $f$  be near 93 MeV, the term  $[(f - 93)/0.02]^2$  was added to the  $\chi^2$  function. The nine parameters were varied until the  $\chi^2$  was minimized. The search was carried out using MINUIT [22], and some parameters were restricted in the search. The range parameters  $\alpha$  were limited to vary between 300 and 900 MeV. The parameter  $b_0$  was allowed to vary between  $-0.28$  and  $-0.52$   $\text{GeV}^{-1}$ , which corresponds to  $\sigma_{\pi N}$  less than 45 MeV and  $\langle p|\bar{s}s|p\rangle$  greater than zero. It is interesting that for the local potential all the best-fit parameters were within the ranges set. A value of  $b_0 = -0.493$   $\text{GeV}^{-1}$  corresponds to  $\sigma_{\pi N} = 44$  MeV, which turns out to coincide with the empirical analysis [12].

Table 3

Best-fit values for  $b_0$  and the double-derivative “ $d$ ” coefficients for both the local and separable potentials. For the local potential, a common range parameter  $\alpha = 0.412$  GeV for all diagonal and off-diagonal channels produced a good fit to the data. All Lagrangian parameters are in  $\text{GeV}^{-1}$ . The range parameters are in GeV

Potential	$b_0$	$d_0$	$d_D$	$d_F$	$d_1$	$d_2$	$\alpha_{\Sigma\pi}$	$\alpha_{\Lambda\pi}$	$\alpha_{\text{KN}}$
local	-0.493	-0.66	-0.02	-0.29	+0.23	-0.39	0.41	0.41	0.41
separable	-0.279	-0.40	-0.24	-0.43	+0.28	-0.62	0.45	0.30	0.76

#### 4. Discussion

Satisfactory fits were found for both the local and separable potentials using appropriate range parameterizations. For the separable potential, the best fit was found using three different ranges for the  $\pi\Sigma$ ,  $\pi\Lambda$ , and  $\bar{K}N$  channels. For the local potential a good fit is obtained using only one common range for all channels. The values of the “best-fit” parameters for the two cases are listed in Table 3. In Table 4 we list the  $\chi^2/N$  for the scattering data along with the values for the threshold branching ratios. In Fig. 1 we plot the total cross sections to the various channels, as well as the  $\Sigma\pi$  mass spectrum for the two fits. The total  $\chi^2$  can be slightly improved for the local potential by using three different ranges as in the separable case. However, the Lagrangian parameters do not change significantly. Thus, we focus our attention on the single range fit, since it reproduces the data well and has the least number of parameters. Also, the preferred value  $\alpha = 412$  MeV lies between the mass of a vector meson and that of two pions. This value is in line with the physics of the process, since such t-channel exchanges are believed to dominate the interaction.

As can be seen from Table 3, the Lagrangian parameters turn out to be very similar for both the local and separable potential fits. This is probably because the range of energies investigated here is small, and thus the results are not sensitive to the form of the potentials. If other potential forms were used, similar values for the Lagrangian parameters would probably be obtained. Thus, the most important parameters in the

Table 4

Best-fit results of the threshold branching ratios Eqs. (21) for both the local and the separable potentials. The  $\chi^2$  per data point is only for the  $K^-p$  elastic and inelastic scattering data. The parameters of the “best fit” are from Table 3

Potential	$f$ (MeV)	$\chi^2/N$	$\gamma$	$R_c$	$R_n$
local	93	1.6	2.30	0.66	0.17
separable	93	2.8	2.26	0.66	0.16
experiment			2.36 $\pm 0.04$	0.66 $\pm 0.011$	0.19 $\pm 0.015$

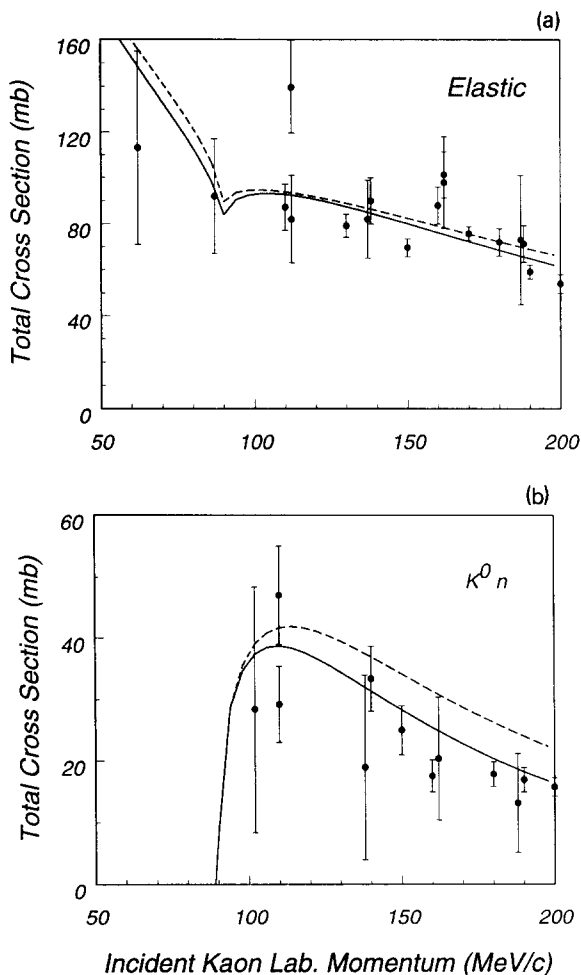


Fig. 1. Calculated cross sections and resonance spectrum compared with experimental data [13–17]: (a)  $K^-p$  elastic scattering, (b)  $K^-p \rightarrow K^0n$ , (c)  $K^-p \rightarrow \pi^0\Lambda$ , (d)  $K^-p \rightarrow \pi^+\Sigma^-$ , (e)  $K^-p \rightarrow \pi^0\Sigma^0$ , (f)  $K^-p \rightarrow \pi^-\Sigma^+$ , and (g) the  $\Sigma\pi$  mass spectrum. The solid curves correspond to the best fit parameters for the local potential, and the dashed curve to the separable potential.

fit are  $b_0$  and the  $d$ 's<sup>3</sup>. To our knowledge, our results are the first estimates of the double-derivative “ $d$ ” parameters.

Although there are six Lagrangian parameters, their freedom to vary is restricted. The parameter  $b_0$  is confined to stay between  $-0.52$  and  $-0.28 \text{ GeV}^{-1}$  as discussed above. Requiring  $a_{\pi N}^+$  and  $a_{KN}^0$  to be near zero reduces the effective degrees of freedom to three. Thus, a fit to the diversified data of the  $\bar{K}N$  system with only one common range parameter (for the local potential) is remarkable. As can be seen in Table 3, the double-derivative “ $d$ ” parameters are mostly negative. The negative sign is needed

<sup>3</sup> Note that possible differences in  $b_0$  related to the  $\pi N$  and  $KN$  sigma terms are compensated by corresponding changes in the  $d$  parameters.

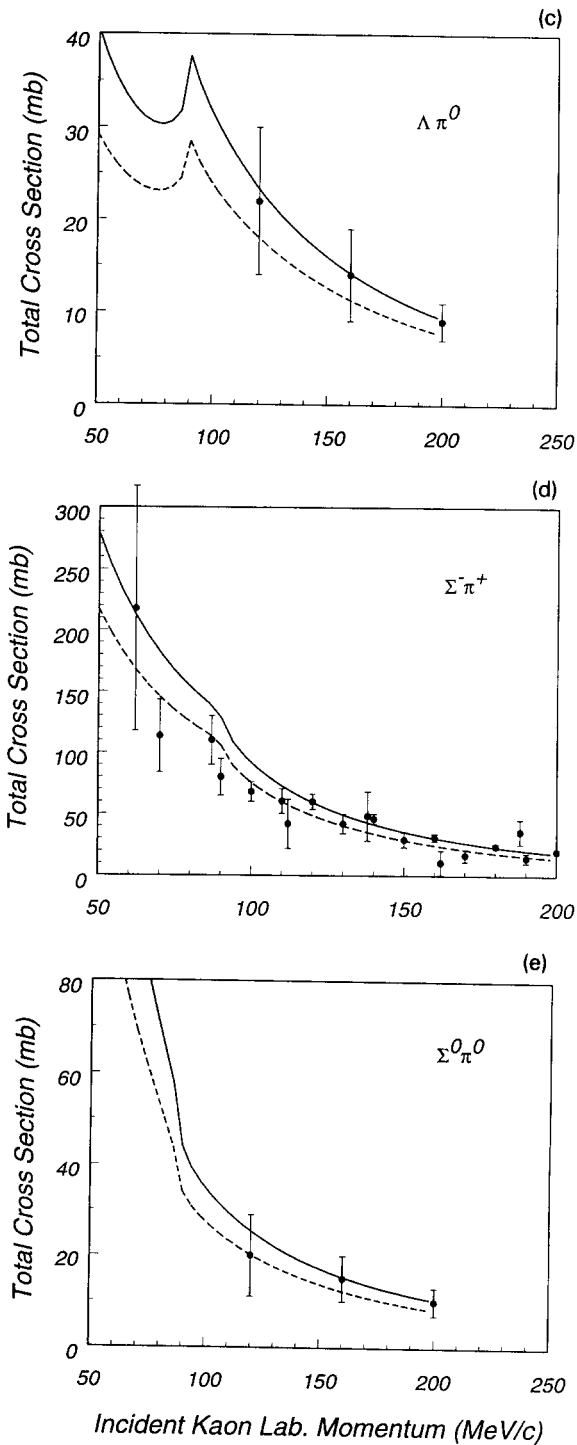


Fig. 1 — continued.

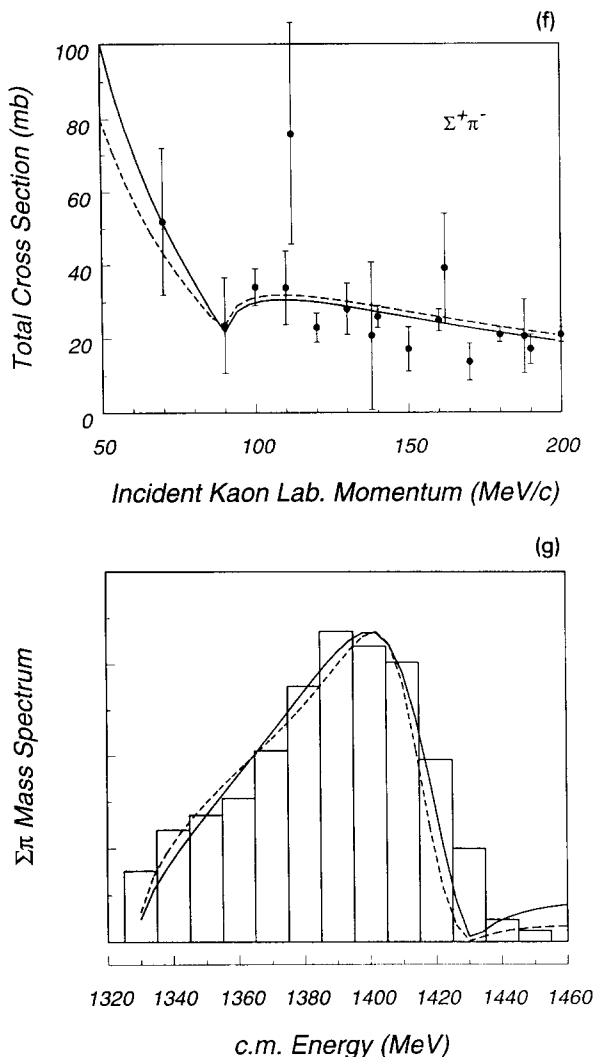


Fig. 1 — continued.

to cancel the quark mass “*b*” terms in  $a_{\pi N}^+$  and  $a_{KN}^0$  in order to obtain the near-zero experimental values of these quantities (see Appendix B). This same cancelation is also desirable in the  $\bar{K}N$  system, since the iterated current algebra term by itself does a fairly good job at fitting the data.

For the  $K^+N$  system, the  $I = 0$  scattering length was incorporated in the fit and is near zero. The scattering length remains essentially zero when the potential is iterated. The “best-fit” parameters also apply to the  $K^+N$  interaction in the  $I = 1$  channel, where the experimental value of the scattering length is  $-0.31 \pm 0.02$  fm [21]. For the local potential, the  $I = 1$  potential is given by Eq. (15) with the  $C_{ij}$  replaced by the  $C_{K^+p \rightarrow K^+p}$  from Appendix B. The Born scattering length for the “best-fit” parameters gives  $-0.49$  fm, and iteration of the potential reduces this value. Thus by choosing an appropriate

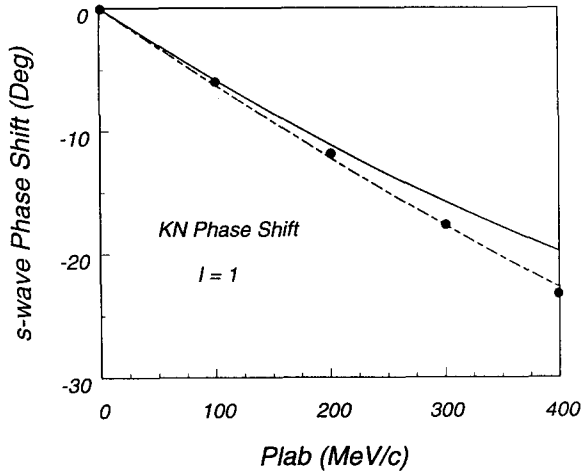


Fig. 2. The  $I = 1$   $K^+N$  (i.e.  $K^+p$ ) phase shift as a function of kaon laboratory momentum. The solid line corresponds to the best-fit using only one common range parameter ( $\alpha = 412$  MeV) for the local potential. A value of  $\alpha_{K^+p} = 500$  MeV reproduces the experimental value of the  $K^+p$  scattering length. The dashed line corresponds to a three parameter fit for the local potential with a larger value for  $\alpha_{KN}$  as mentioned in the text. In this case,  $\alpha_{K^+p}$  is equal to 760 MeV. The dots are from the phase shift analysis of Martin [23].

range for this channel, the scattering length can be made equal to the experimental result. A range parameter of  $\alpha_{K^+p} = 500$  MeV reproduced the experimental value of  $-0.31$  fm. We note that this range also gives reasonable agreement with the energy dependence of the  $I = 1$  s-wave phase shift as shown in Fig. 2. Here we plot the s-wave phase shift as a function of kaon laboratory momentum for this fit by the solid line. The dots correspond to the phase shift taken from Ref. [23].

We have investigated if there were any other satisfactory fits to the data by using different starting points for the search. We also tried three different ranges with the local potential, and found one fit with  $\alpha = 569$  MeV for the  $\bar{K}N$  channel, but with very similar values for the Lagrangian parameters as in Table 3. In Fig. 2 we plot the s-wave  $K^+p$  phase shift for this fit by the dashed line. In this case,  $\alpha_{K^+p} = 760$  MeV, and the energy dependence agrees even better with Martin's phases [23]. The overall best fit used three ranges for the local potential and produced a  $\chi^2/N = 1.7$  for all the data, but again with similar values for the Lagrangian parameters.

We note that the parameters were fitted to the data using a potential model, and need to be interpreted in this context. We briefly comment on possible limitations of the potential model approach when comparing with a chiral perturbation expansion.

When iterating the potential in the Lippmann–Schwinger equation, four-dimensional loop integrals are not calculated in all completeness. The energy part of the integral is integrated out, producing a propagator appropriate for the three remaining dimensions. All multiple scatterings include only “ladder” graphs. Crossed graphs are not included in our calculation in the iteration process, and the meson–meson interaction is neglected. This is expected to be a reasonable approximation, since the energies are low, the mass of the kaon is relatively large, and the resonance at 1405 MeV dominates the  $\bar{K}N$  interaction

at low energies. The S-matrix we obtain in the potential model is unitary, and has a pole at the  $\Lambda(1405)$  resonance. The Born amplitudes respect crossing symmetry, but the full amplitudes cannot be extended too far in energy away from the region investigated here, since neglecting crossed graphs in the iteration of the potential violates crossing symmetry. It is encouraging, however, that the s-wave  $K^+p$  scattering length and the energy dependence of the phase shift are reproduced reasonably well even though only the Born amplitudes respect crossing symmetry.

In a systematic chiral perturbation expansion, amplitudes are expanded in powers of meson energies. The terms up to order  $q^2$  for s-wave scattering are given entirely in terms of the current algebra term, the “ $b$ ” and “ $d$ ” parameters and relativistic corrections to order  $q^2$ . The  $q^3$  contribution is given by single loops involving just the current algebra term and higher order counter terms. However, using a potential model with a cutoff introduces an additional length scale. This is most easily seen by examining the separable potential for which an analytic solution exists. For a single channel separable potential, the scattering amplitude is given by

$$f_{K^+p} = f_{\text{Born}} \left[ 1 + f_{\text{Born}} \left( \frac{k^2 - \alpha^2}{2\alpha} - ik \right) \right]^{-1}, \quad (22)$$

and the scattering length is thus

$$a = a_{\text{Born}} \left( 1 - \frac{1}{2} \alpha a_{\text{Born}} \right)^{-1}. \quad (23)$$

Here  $a_{\text{Born}}$  includes both the current algebra term (order  $q$ ) and the tree level terms of order  $q^2$ . By expanding the denominator, the next power of “ $q$ ” after  $q^2$  is  $q^2\alpha$ . Thus, it is not possible to compare terms from the potential model used here with those of a chiral perturbation expansion beyond order  $q^2$ . However, one can use the above equation to estimate how a chiral perturbation series might converge for the  $K^+p$  s-wave scattering amplitude. To order  $q$  the scattering length is  $-0.59$  fm. Using the “best-fit” parameters of the separable potential, the  $q^2$  terms contribute  $-0.11$  fm to the scattering length. Thus  $a_{\text{Born}} = -0.70$  fm. Order  $q^3$  and higher terms need to be large to bring the scattering length close to the experimental value. For the separable potential one can calculate the contribution of the once iterated current algebra piece, which in a chiral perturbation expansion is the  $q^3$  term. To obtain  $a_{K^+p} \simeq -0.3$  fm, the experimental value, one needs  $\alpha_{K^+p} = 667$  MeV, making the  $q^2\alpha$  term equal to  $+0.58$  fm. Thus, we see here that the once iterated current algebra term can be as large the order  $q$  term.

Eq. (23) is instructive in comparing the difference between the  $S = +1$  and  $S = -1$  KN interactions. The current algebra terms have opposite sign, negative for  $K^+p$  and positive for  $K^-p$ . For the  $K^+p$  case ( $a_{\text{Born}} < 0$ ) the multiple scattering reduces the scattering length from the Born result in accord with experiment. Since  $a_{\text{Born}}$  is roughly twice the experimental value, a short range (large  $\alpha$ ) is needed for the multiple scattering to produce a large enough correction. This short range is also desirable in obtaining the correct energy dependence of the s-wave phase shift, for which there is a small effective range. For the  $K^-p$  case ( $a_{\text{Born}} > 0$ ), the multiple scattering causes a zero in the denominator producing a quasi-bound state.

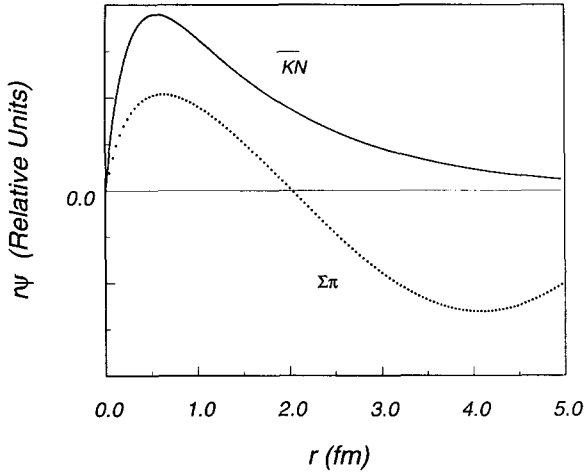


Fig. 3. Radial wave functions  $u(r) = r\Psi(r)$  for the  $\bar{K}N$  and  $\pi\Sigma$   $I = 0$  channel at  $\sqrt{s} = 1405$  MeV are plotted as a function of the relative coordinate  $r$ .

The  $\Lambda(1405)$  produced in the potential model derived here is a bound state in the  $\bar{K}N$  ( $I = 0$ ) channel and a resonance in the  $\pi\Sigma$  channel. It is instructive to verify this in terms of the  $\bar{K}N$  and  $\pi\Sigma$  wave functions. In Fig. 3 we plot these wave functions, taken at the energy corresponding to the peak of the  $\pi\Sigma$  mass spectrum, for the best-fit one-parameter local potential (i.e. with  $\alpha = 412$  MeV). The horizontal axis is the  $\bar{K}N$  or  $\pi\Sigma$  relative coordinate  $r$ , and the vertical axis is the radial wave function  $u(r) = r\Psi(r)$ . The root mean square radius of the  $\bar{K}N$  bound state is 1.3 fm.

Historically there has been a disagreement between the scattering length extracted from the scattering data versus the  $K^-p$  1s atomic level shift. In our analysis as well, the real part has the opposite sign as the atomic level shift results. In Fig. 4 we plot the

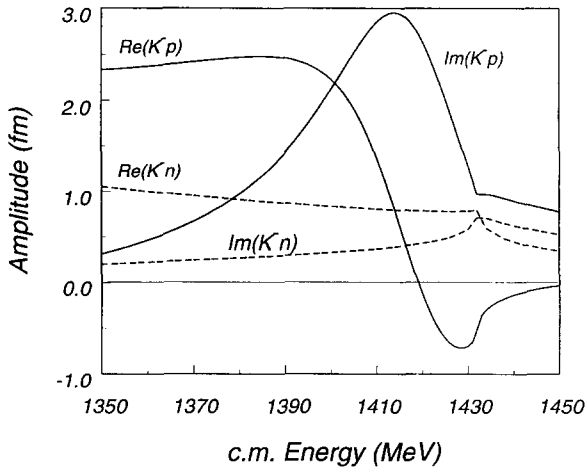


Fig. 4. The  $I = 0$  and 1 scattering amplitudes for the  $\bar{K}N$  system at and below the  $K^-p$  threshold.



real and imaginary part of the scattering amplitude near and below the  $K^-p$  threshold for both the local and separable potential. The structure below threshold is typical of a resonance. The  $K^-p$  scattering length we obtain is  $-0.97 + 1.1i$  fm, and in the isospin limit setting  $m_K = m_{\bar{K}^0}$  and  $M_p = M_n$  we get  $-0.51 + 0.89i$  fm. The experimental data is still controversial [21], so we did not include it in our fits. It is important to obtain a reliable value for the level shift, since if further experimental analysis confirms earlier results, chiral dynamics will be in disagreement with the data. In general, more scattering data would also be useful in further testing the predictions based on chiral dynamics, since the experimental data for the scattering channels are quite old, and for some channels not very extensive.

## 5. Conclusions

We have applied the effective chiral Lagrangian to the strangeness  $S = -1$  sector of the  $\bar{K}N$  interaction by constructing a pseudo-potential from the Lagrangian, such that this potential used in the Born approximation has the same  $s$ -wave scattering length as the chiral Lagrangian up to order  $q^2$ . This potential model approach successfully produces the  $\Lambda(1405)$  resonance just below the  $K^-p$  threshold. A number of Lagrangian parameters were adjusted to fit the available low-energy  $\bar{K}N$  data, with constraints from the  $S = +1$   $KN$  system and the isospin-even  $\pi N$  scattering length. Satisfactory results were found using both local and separable potential forms, and a good fit was obtained using only one common range parameter for all channels in the local potential. The Lagrangian parameters turned out roughly the same for both potential forms used. To our knowledge the values obtained here are the first estimates of some of these parameters.

## Acknowledgements

During the final preparation of this paper, one of us (W.W.) enjoyed stimulating discussions with G.E. Brown, J. Gasser, B. Holstein, D. Kaplan, Ch. Pethick, and M. Rho at the INT, Seattle in the course of the program “Chiral Dynamics of Hadrons and Nuclei”. One of us (P.S.) would like to thank the Physics Department at the Technische Universität München for the hospitality extended to him during his sabbatical stay.

## Appendix A

The pseudoscalar meson field matrix  $\phi$  from Eq. (4) is given by

$$\phi = \sqrt{2} \begin{pmatrix} \frac{\eta_8}{\sqrt{6}} + \frac{\pi^0}{\sqrt{2}} & \pi^+ & K^+ \\ \pi^- & \frac{\eta_8}{\sqrt{6}} - \frac{\pi^0}{\sqrt{2}} & K^0 \\ K^- & \bar{K}^0 & -\frac{2}{\sqrt{6}}\eta_8 \end{pmatrix} \quad (\text{A.1})$$

and the baryon matrix  $B$  is

$$B = \begin{pmatrix} \frac{\Lambda}{\sqrt{6}} + \frac{\Sigma^0}{\sqrt{2}} & \Sigma^+ & p \\ \Sigma^- & \frac{\Lambda}{\sqrt{6}} - \frac{\Sigma^0}{\sqrt{2}} & n \\ \Xi^- & \bar{\Xi}^0 & -\frac{2}{\sqrt{6}}\Lambda \end{pmatrix}. \quad (\text{A.2})$$

Using the Gell-Mann, Oakes, Renner (GOR) relation in the isospin limit for the pseudoscalar mesons, the mass matrix  $\chi$  is given by

$$\chi = \begin{pmatrix} m_\pi^2 & 0 & 0 \\ 0 & m_\pi^2 & 0 \\ 0 & 0 & 2m_K^2 - m_\pi^2 \end{pmatrix}. \quad (\text{A.3})$$

## Appendix B

Here we list the values of the relative coupling strengths  $C_{ij}$  for the potential of Eqs. (12), (15), (16) in terms of the parameters of the chiral Lagrangian. Channel one corresponds to the  $\pi^+\Sigma^-$  state, channel two to  $\pi^0\Sigma^0$ , channel three to  $\pi^-\Sigma^+$ , channel four to  $\pi^0\Lambda$ , channel five to  $K^-p$ , and channel six to the  $\bar{K}^0n$  state:

$$C_{11} = -E'_\pi + (F^2 + \frac{1}{3}D^2) S_{\pi\pi} + 4m_\pi^2 (b_D + b_0) - E_\pi^2 (2d_D + 2d_0 + d_1),$$

$$C_{12} = -E'_\pi + \frac{1}{3}D^2 S_{\pi\pi} - F^2 U_{\pi\pi} - E_\pi^2 (d_1 + d_2),$$

$$C_{13} = -2E_\pi^2 (d_1 + d_2) + (\frac{1}{3}D^2 - F^2) (S_{\pi\pi} + U_{\pi\pi}),$$

$$C_{14} = \frac{DF}{\sqrt{3}} (S_{\pi\pi} - U_{\pi\pi}),$$

$$C_{15} = -(F^2 + \frac{1}{3}D^2) \frac{1}{2} S_{\pi K} + (D^2 - F^2) \frac{1}{2} U_{\pi K} - E_K E_\pi (d_1 + d_2),$$

$$C_{16} = -\frac{1}{4}(E'_\pi + E'_K) + (\frac{1}{2}F^2 - DF - \frac{1}{6}D^2) S_{\pi K} \\ - (m_\pi^2 + m_K^2)(b_F - b_D) - E_\pi E_K (d_D - d_F + d_1)$$

$$C_{22} = C_{11} - C_{12} + C_{13},$$

$$C_{23} = C_{12},$$

$$\begin{aligned}
 C_{24} &= 0, \\
 C_{25} &= \frac{1}{2}(C_{15} + C_{16}), \\
 C_{26} &= C_{25}, \\
 C_{33} &= C_{11}, \\
 C_{34} &= -C_{14}, \\
 C_{35} &= C_{16}, \\
 C_{36} &= C_{15}, \\
 C_{44} &= \frac{1}{3}D^2 (S_{\pi\pi} + U_{\pi\pi}) + 4m_\pi^2 (b_0 + \frac{1}{3}b_D) - E_\pi^2 (2d_0 + \frac{1}{3}2d_D + \frac{1}{3}d_2), \\
 C_{45} &= -\frac{1}{8}\sqrt{3}(E'_\pi + E'_K) + \frac{D}{2\sqrt{3}}(D - F) S_{\pi K} - \frac{1}{4}\sqrt{3}(D + F) (\frac{1}{3}D + F) U_{\pi K} \\
 &\quad - \frac{1}{2\sqrt{3}} (m_\pi^2 + m_K^2)(b_D + 3b_F) + \frac{1}{2\sqrt{3}} E_\pi E_K (d_D + 3d_F - d_2), \\
 C_{46} &= -C_{45}, \\
 C_{55} &= -E'_K + (F^2 + \frac{1}{3}D^2) S_{KK} + 4m_K^2 (b_D + b_0) - E_K^2 (2d_D + 2d_0 + d_1), \\
 C_{56} &= -\frac{1}{2}E'_K + (\frac{1}{2}F^2 + DF - \frac{1}{6}D^2) S_{KK} + 2m_K^2 (b_D + b_F) - E_K^2 (d_D + d_F + d_1), \\
 C_{66} &= C_{55},
 \end{aligned} \tag{B.1}$$

where  $E_\pi$  and  $E_K$  denote the pion and kaon energy, respectively, in the center-of-mass frame. The pion and kaon masses are labeled as  $m_\pi$  and  $m_K$ . The quantities labeled  $E'_\pi$  and  $E'_K$  include the relativistic correction to the current algebra piece to order  $q^2$  and are

$$E'_\alpha = E_\alpha + \frac{E_\alpha^2 - m_\alpha^2}{2M_0}. \tag{B.2}$$

The quantities  $S_{\alpha\beta}$  and  $U_{\alpha\beta}$  are defined as

$$S_{\alpha\beta} = \frac{E_\alpha E_\beta}{2M_0}, \tag{B.3}$$

$$U_{\alpha\beta} = \frac{1}{3M_0} \left( 2m_\alpha^2 + 2m_\beta^2 + \frac{m_\alpha^2 m_\beta^2}{E_\alpha E_\beta} - \frac{7}{2} E_\alpha E_\beta \right), \tag{B.4}$$

where the index  $\alpha$  (or  $\beta$ ) stands for pion or kaon. These terms arise from the Born graphs involving the axial vector couplings which have an octet baryon exchanged in the “s”- or “u”-channel.  $M_0$  is the baryon octet mass in the chiral limit which we take as 910 MeV. Note that  $C_{ij} = C_{ji}$ .

The  $1/E$  terms in  $U_{\alpha\beta}$  deserve some explanation. Baryon exchange in the u-channel leads to logarithmic singularities in the partial wave amplitudes below threshold. In the  $\pi N$  case it gives rise to the so-called short nucleon cut [24] extending from  $s = (M_N - m_\pi^2/M_N)^2$  to  $s = M_N^2 + 2m_\pi^2$ . In the heavy mass limit, both logarithmic branch points in the  $E_\pi$ -plane coalesce and give rise to a pole singularity. The presence of subthreshold singularities restricts the kinematic range for the potential approach to

be applied. In this analysis the energies are well above these singularities; the nearest coming from  $\pi\Sigma \rightarrow \bar{K}N$  is located at  $\sqrt{s} = 1.24$  GeV ( $E_\pi = 58$  MeV). Even if one used the full expression for the u-channel exchange (producing logarithmic singularities) instead of the heavy mass limit to order  $q^2$  (producing pole singularities very close to the logarithmic ones) the results of the analysis would not change. In fact, when we neglected the s- and u-channel baryon exchange amplitudes entirely, we obtained a good fit to the data with similar values for  $b_0$  and the “d” parameters as in Table 3.

The potential strength for the  $I = 1$  channel for  $K^+N$  scattering (i.e.  $K^+p$  scattering) is given by

$$C_{K^+p \rightarrow K^+p} = E_K + \frac{E_K^2 - m_K^2}{2M_0} + (F^2 + \frac{1}{3}D^2) U_{KK} + 4m_K^2 (b_0 + b_D) - E_K^2 (2d_D + 2d_0 + d_1). \quad (\text{B.5})$$

In terms of the Lagrangian parameters, the  $\pi N$  isospin-even scattering length to order  $q^3$  is given by [25]

$$a_{\pi N}^+ = \frac{1}{4\pi(1 + m_\pi/M_N)} \times \left[ \frac{m_\pi^2}{f^2} \left( -2b_D - 2b_F - 4b_0 + d_D + d_F + 2d_0 - \frac{g_A^2}{4M_N} \right) + \frac{3g_A^2 m_\pi^3}{64\pi f^4} \right], \quad (\text{B.6})$$

where  $g_A$  is the axial vector coupling constant. The experimental value of the even  $\pi N$  scattering length is  $-0.012 \pm 0.006$  fm [20]. The  $I = 0$  for the strangeness  $S = +1$  KN interaction is given to order  $q^2$  (i.e. tree level) as

$$a_{KN}^0 = \frac{1}{4\pi(1 + m_K/M_N)} \times \frac{m_K^2}{f^2} \left[ 4b_0 - 4b_F + 2d_F - 2d_0 + d_1 + \frac{D}{M_N} \left( F - \frac{1}{3}D \right) \right]. \quad (\text{B.7})$$

The experimental value for this quantity is  $-(0.02 \pm 0.04)$  fm [21].

## References

- [1] For some recent reviews, see G. Ecker, *Prog. Part. Nucl. Phys.* 35 (1995) 1; V. Bernard, N. Kaiser and U.-G. Meißner, *Int. J. Mod. Phys. E* 4 (1995) 193.
- [2] C.-H. Lee, H. Jung, D.-P. Min and M. Rho, *Phys. Lett. B* 326 (1994) 14.
- [3] G.E. Brown, C.-H. Lee, M. Rho and V. Thorsson, *Nucl. Phys. A* 567 (1993) 937.
- [4] R.H. Dalitz, T.-C. Wong and G. Rajasekaran, *Phys. Rev.* 153 (1967) 1617; E.A. Veit, B.K. Jennings, A.W. Thomas and R.C. Barrett, *Phys. Rev. D* 31 (1985) 1033; P.B. Siegel and W. Weise, *Phys. Rev. C* 38 (1988) 2221.
- [5] J. Gasser, M.E. Sainio and A. Svarc, *Nucl. Phys. B* 307 (1988) 779.
- [6] A. Krause, *Helv. Phys. Acta* 63 (1990) 3.
- [7] J. Gasser and H. Leutwyler, *Nucl. Phys. B* 250 (1985) 465.
- [8] M. Bourquin et al., *Z. Phys. C* 21 (1983) 27.
- [9] E. Jenkins and A.V. Manohar, *Phys. Lett. B* 255 (1991) 558.
- [10] V. Bernard, N. Kaiser and U.-G. Meißner, *Z. Phys. C* 60 (1993) 111.

- [11] S. Weinberg, *Phys. Rev.* 166 (1968) 1568.
- [12] J. Gasser, H. Leutwyler and M.E. Sainio, *Phys. Lett. B* 253 (1985) 252, 260.
- [13] J. Ciborowski et al., *J. Phys. G* 8 (1982) 13.
- [14] D. Evans et al., *J. Phys. G* 9 (1983) 885.
- [15] W.E. Humphrey and R.R. Ross, *Phys. Rev.* 127 (1962) 1305.
- [16] J.K. Kim, Columbia University Report, Nevis 149 (1966).
- [17] M. Sakitt et al., *Phys. Rev.* 139 (1965) 719.
- [18] R.J. Nowak et al., *Nucl. Phys. B* 139 (1978) 61.
- [19] D.N. Tovee et al., *Nucl. Phys. B* 33 (1971) 493.
- [20] R. Koch, *Nucl. Phys. A* 448 (1986) 707.
- [21] For a compilation of the scattering lengths, see C. Dover and G. Walker, *Phys. Reports* 89 (1982) 1.
- [22] F. James, in: *Proc. 1972 CERN Computing and Data Processing School, Pertisan, Austria, 1972*, CERN Report 72-21;  
F. James and M. Roos, MINUIT functional minimization and error analysis, D506-Minuit, CERN (1989).
- [23] A.D. Martin, *Nucl. Phys. B* 94 (1975) 413.
- [24] G. Höhler, in: *Landolt-Börnstein*, vol. 9b2, ed. H. Schopper (Springer, Berlin, 1983) Appendix A7.
- [25] V. Bernard, N. Kaiser and U.-G. Meißner, *Phys. Lett. B* 309 (1993) 421.